UNIVERSITY OF CALIFORNIA
RIVERSIDE

Effects of Estrogen Receptor Beta (ERβ) Ligand Treatment on Purkinje Neuron Dysfunction in an EAE Mouse Model

A Thesis submitted in partial satisfaction
of the requirements for the degree of

Master of Science

in

Biomedical Sciences

by

Oluwadara Ogundare

December 2023

Thesis Committee:
Dr. Seema Tiwari-Woodruff, Chairperson
Dr. David Lo
Dr. Emma Wilson

The Thesis of Oluwadara Ogundare is approved:

Committee Chairperson

University of California, Riverside

DEDICATION

For my family, my friends, my people, and my person. I could not have done this without you. AML

ABSTRACT OF THE THESIS

Effects of Estrogen Receptor Beta (ERβ) Ligand Treatment on Purkinje Neuron Dysfunction in an EAE Mouse Model

by

Oluwadara Ogundare

Master of Science, Graduate Program in Biomedical Sciences
University of California, Riverside, December 2023
Dr. Seema Tiwari-Woodruff, Chairperson

Multiple sclerosis is a chronic demyelinating disease of the central nervous system. Patients with Ms. See a range of symptoms including cognitive dysfunction, vision problems, as well as symptoms of cerebellar ataxia. Previous studies have shown both Purkinje cell and mitochondrial dysfunction due to the demyelination seen in multiple sclerosis. This study aims to analyze the direct or indirect effect of an estrogen receptor beta ligand and usual chloride O methyl. Unfortunately, due to poor tissue quality the results from this study are inconclusive and must be repeated. Regardless, this study creates a basis of information for further research to expand upon.

TABLE OF CONTENTS

LIST OF FIGURES

LIST OF TABLES

Chapter 1: Introduction

Multiple Sclerosis

Multiple sclerosis (MS) is an autoimmune, demyelinating, neurodegenerative disease of the central nervous system (CNS).[1] As of 2020, there are approximately 2.8 million people worldwide.[2] People with XX chromosomes are on average two to four times as likely to develop symptoms of MS compared to those with XY chromosomes, which can be seen as early as the mid-20s[2]. On a molecular level, MS is characterized by infiltration of peripheral immune cells such as T and B lymphocytes as well as by demyelination and axon damage[1]. Autoreactive T and B cells are activated in the peripheral lymph nodes and differentiate into effector cells, and travel through the blood into the brain which is one of the earliest indications of disease[1]. Once in the CNS these cells activate B cells and are further activated by antigen presenting cells[1]. The activated macrophages and effector cells (CD4+ and CD8+ T cells) cause damage to CNS cells by breaking down the myelin components as well as produce cytokines and chemokines that gather other autoreactive cells from the periphery[1]. This increased inflammation in the CNS causes additional demyelination and axonal damage[1] that has numerous clinical effects on patients including musculoskeletal weakness and cognitive dysfunction, spasticity, vision, and sensory loss as well as symptoms of cerebellar ataxia like gait instability. [3]

Cerebellum

The Cerebellum is one of the major structures of the CNS. It aids in motor movement regulation as well as aiding in coordination of balance, equilibrium movement, and motor learning.[4] Structurally the cerebellum has two hemispheres that are divided into three different lobes, which are separated by two main fissures, the primary and posterior fissure[4]. The primary fissure separates the anterior and posterior lobes, while the posterior fissure separates the posterior and flocculonodular lobes.[4] The cerebellar cortex can then be further divided into the cerebrocerebellar, the spinocerebellar and the vestibulocerebellar tracts [5] . The cerebellum has a dense population of neurons that are divided into three main layers, the innermost granule cell layer, the middle Purkinje cell layer, and the external molecular layer. The granule cells of the cerebellum give rise to parallel fibers that synapse with the dendrites of the PCs within the molecular layer[5]. The molecular layer also contains basket and stellate cells (interneurons that aid in cerebellar cortex output control)[4]. Purkinje neurons (PC) are heavily myelinated neurons that form the single output of the cerebellum and are GABA-energic in nature[5]. PCs receive inputs from the parallel fibers, as well as direct modulatory input from the climbing fibers [5]. PC axons synapse onto the deep cerebellar nuclei and generate error correction signals that can modify active movement [5]. The Purkinje cell (PC) plays a major role in motor coordination, fine motor control, as well as course-correction in movement[5]. Purkinje cell circuitry is as follows: Excitatory signals from the pontine nuclei (and inferior olive) travel to the granule cell layer via mossy fibers which arise from the motor cortex and the spinal cord.[5] The mossy fibers synapse

onto the granule cells which in form turn into the parallel fibers which synapse with the PC dendrites in the molecular layer[6]. This positive signal activates the PCs which send inhibitory signals back down to the deep cerebellar nuclei[6]. In general, the cerebellum controls the body ipsilaterally[5]. The cerebellum follows two main pathways, the efferent cerebello-thalamo-cortical (CTC) pathway and the afferent cortico-ponto-cerebellar (CPC) pathway [7]. Because of the nature of the work that PC cells do they are incredibly large cells that require high levels of energy[8].

Cerebellar Pathology in MS

Dysfunction of the cerebellum can cause a multitude of symptoms in the case of MS including limb, gait, and truncal ataxia, dysarthria, and tremors[9]. Ataxia causes poor muscle control that causes clumsy voluntary movements[10]. Approximately 80% of patients have one of three main types of ataxias (cerebellar, sensory, and vestibular) with cerebellar being the most common[9]. This results in difficulty with walking and balance, hand coordination, speech and swallowing as well as eye movement in patients with MS[9]. This ataxia is caused by the formation of lesions in the cerebellum of affected patients[9]. White matter lesions (areas of damage or scarring) of the cerebellum are most seen in the cerebellar peduncles[9]. The cerebellar dysfunction symptoms seen in MS can be linked to functional cerebellar degeneration, more specifically PC demyelination and loss [9]. The lesions reduce the overall cerebellar volume due to the breakdown of the myelin that normally covers neurons in the CNS[9]. The degredation of the myelin causes alterations in mitochondrial dynamics to compensate for the inefficiencies in synaptic messaging [8].

This indicates a great need to understand the structural and molecular breakdown of the cerebellum, its cells, as well as the mitochondrial dysfunction seen in MS pathology.

Mitochondria

Mitochondria play an important role in cellular energetics[11] and are the main source of cellular ATP. Mitochondria have functional inner and outer membrane divided by the intermembrane space[11]. The mitochondria house the electron transport chain in the inner membrane[11]. This important cellular complex creates ATP using four main protein complexes (I-IV) and ATP synthase[11]. The structure of the mitochondria allows for the creation of a proton gradient in the intermembrane space by the proton pump action of three of the four protein complexes (I, III, and IV)[12]. Complexes I and III create byproducts called reactive oxygen species (ROS)[13]. Changes in ROS levels can result in damage to the cells due to their role in normal cell functioning[13].The fourth protein complex, the cytochrome c oxidase (COX) complex IV, is vital for apoptosis and can be used as a biomarker for mitochondria in immunohistochemistry studies of MS tissue[12,14].

Mitochondrial Dysfunction in MS

Mitochondrial dysfunction is seen in many degenerative diseases[15]. Tissue samples from MS patients as well as experimental autoimmune encephalomyelitis (EAE) mouse models, have shown increased mutations in mitochondrial DNA, impaired mitochondrial gene expression as well as defective mitochondrial enzymes[13]. Dysfunctional mitochondrial cause an increase in cellular oxidative stress via the production of free

radicals (a type of ROS)[16,17]. ROS can be detrimental to the macromolecules that makeup the neuronal system[13]. Mitochondrial dysfunction also disturbs the delicate metabolic pathways which causes imbalances of neurotrophic substances that enable the survival of oligodendrocytes and neurons[13]. Without functional oligodendrocytes, the neuronal axons will become demyelinated[13].This demyelination influences the energetic needs of a neuronal cell. In order to compensate for the energetic demands, mitochondria can undergo fission or fusion to aid in regulation of the number, morphology, and position changes within the cell[8]. Mitochondrial transport and docking are a dynamic process that changes based on the energetic needs of the cell[18]. Syntaphilin acts as an anchor for mitochondria and plays a vital role in increasing mitochondrial station sites in demyelinating axons[18]. These station sites help the cell maintain a higher volume of mitochondria where they are needed (lesioned areas)[18]

Mouse models of Multiple Sclerosis

As it stands, there are many difficulties in studying the onset and progression of MS in humans, due in part to the inability to collect tissue patients, as well as the range of symptoms different patients can experience[19]. To study disease progression multiple mouse models have been studied and two main ones are used. The cuprizone model has been shown to create an increase in oxidative stress leading to oligodendrocyte apoptosis as well as microgliosis and astrogliosis[20]. Cuprizone is a copper chelating agent that strictly causes demyelination in the multiple sclerosis model [20]. The other model representing MS is experimental autoimmune encephalomyelitis (EAE). EAE can be

induced by immunization of one of a specific myelin peptide emulsified with an adjuvant [21]. Different peptides paired with different mouse strains mimic different clinical forms of MS[21]. The Tiwari-Woodruff EAE uses a short peptide of the myelin oligodendrocyte glycoprotein (MOG) protein (peptide 35-55) and Mycobacterium tuberculosis emulsified in complete Freud's Adjuvant (CFA). This was paired with injection of pertussis toxin in C57BL/6 mice to create a monophasic chronic disease phase with peak disease occurring around the 21st day post injection [21] .This model shows both CNS axon demyelination and perivascular mononuclear infiltration which is more like MS pathology than other models[21]. Previous data has demonstrated marked mitochondrial changes after EAE induction [8]. As earlier stated, mitochondrial changes lead to demyelination of the axons, with this information, the Tiwari-woodruff lab has investigated different remyelinating agents[22]

Estrogen and ERβ ligands

Studies have shown that the rate of relapse decreases during pregnancy, particularly at the 3rd trimester, and increases in the first three months post-partum[23]. Research has also shown that estriol (an estrogen derivative) has neuroprotective effects in EAE treated mice[24]. Most currently approved medications for MS do not aid in repairing damaged myelin, nor do they prevent neurodegeneration[22]. Treatment with an estrogen receptor beta (ERβ) specific ligand, indazole chloride (IndCl) has shown promising effects in decreasing clinical symptoms as well as providing neuroprotection in the MS model of EAE [22].

Preliminary Data

Past studies from the lab have confirmed the use of EAE to create a chronic demyelination model of MS for the longitudinal study of pathology and repair[21]. This study showed consistent MS-like pathology in mice including the consistent loss of PCs and mitochondrial markers from early to late disease progression[21]. Previous work in the Tiwari-Woodruff lab screened seven different analogues of the IndCl molecule and found the IndCl-O-Methyl form to have comparable remyelinating effects as IndCl[22]. The study showed a decrease in PC loss, an increase in COXIV in PC bodies as well as decreases in neuronal pathology post treatment around day 40[21]. However, it is still unknown whether the beta Estrogen receptor plays a direct or indirect role in re-myelination of these PCs. To quantify the changes and modulations in PC neurons given the IndCl-O-Methyl treatment with and without ERβ, we will induce a PC- specific ERβ conditional knock out transgenic mouse model (PCP2Cre + ERβ CKO) with EAE. This mouse model uses the Cre-Lox system to express the Cre recombinase under the control of the Purkinje cell protein (PCP2), which is then crossed with ERβ strain mice which results in mice with Cre-mediated deletion of the flanked ERβ sequence resulting a conditional knockout of ERβ expression in Purkinje neurons. I will test them against a group of wild type (WT) mice. I hypothesize that ERβ ligand treatment will be responsible for the amelioration of EAE (chronic demyelination) induced PC dysfunction. I will test these aims using both mouse lines, split into three groups and induced with their different treatments (normal, EAE+ Vehicle, and EAE+ O-methyl). The animals will be sacrificed on day 40 post injection, cryoprotected, sliced and stained for analysis. I will use immunohistochemistry

stains for myelin basic protein (MBP), COXIV and syntaphilin to determine the treatments effects on the PCs.

Chapter 2: General Methods

Animals

This study followed the protocol established by the American Veterinary Medicine in accordance with the National Institute of Health (NIH) and were approved by the Institutional Animal Care and Use Committee (IACUC) at UCR, Riverside. B6.129-Tg (Pcp2-cre)2Mpin/J female mice were obtained from Jackson Laboratory and crossed with ERβ KO mice, then were maintained in-house at the animal facility. The transgenic litter(s) were verified by PCR for genetic monitoring. Thy-1 YFP and PLP-eGFP female mice were used as a wild-type animal control. Animals were held at five per cage with standard light/dark cycles.

Experimental Autoimmune Encephalomyelitis (EAE)

EAE was induced in eight- to twelve-week-old female C57BL/6J, Thy1-YFP, PLP-eGFP, and PCP2Cre + ERβ CKO mice. The protocol was taken from previous lab work[25,26]. Briefly, the lab EAE protocol is as follows: MOG_{35-55} peptide (300µg/mouse) and Mycobacterium tuberculosis (500µg/mouse) are emulsified in complete Freund's adjuvant (BD Difco, Franklin Lakes, NJ)[25]. Injections of the MOG emulsification is done on Day 0, and day 7 at a volume of 0.1ml/mouse. The injections were placed subcutaneously into the backs of the animals over the right draining inguinal and axillary lymph nodes for the first set of injections and again on the contralateral side for the day 7 injections[25]. The MOG injections were supplemented with an intraperitoneal injection of

Bordetella pertussis toxin (500ng/mouse) (List Biological Laboratories, Campbell, CA) on day 0 and day 2 [25]. Mice were monitored daily starting on day 7 according to a standard EAE clinical disease scoring scale ranging from 0-to 5 increasing in 0.5 increments as described in Hasselman et al, 2017 [21]. A 0 on the scale indicates that when rolled by the tail, the mouse can resist. A clinical score of 1 shows tail limpness with no evidence of muscle weakness, 2 shows no hind limb paralysis but failure to maintain posture when rolled [21]. At a score of 3, the mouse can no longer climb over the edge of the cage, and has partial paralysis of the hind limbs, while a score of 4 shows complete paralysis of both hind limbs[21]. With a clinical EAE score of 5, the mouse is immobile and unresponsive, and immediate euthanasia is recommended[21]. The increase in score is indicative of more lesions forming in the brain and spinal cord[27].

Treatment

During peak EAE disease, a small population of mice (EAE+ Vehicle and EAE+O-methyl) were treated and injected subcutaneously with either the vehicle (90% (vol/vol) Miglyol 812N and 10% ethanol) or IndCl-O-methyl dissolved in the vehicle solution[22]. The mice were injected daily with 5mg/kg body weight of the treatment in a volume of 0.1mL/injection post day 7 immunization of the MOG EAE[28].

Animal groups

There were three different groups per mouse line (Wild type (WT) and PCP2Cre + ERβ CKO); Normal, EAE induced mice (EAE + Vehicle) and EAE induced mice treated with

Estrogen receptor ligand - O-methyl (EAE + O-methyl). Mice were sacrificed on day 40 and were perfused, isolated, and used for immunohistochemistry.

Immunohistochemistry

Immunohistochemistry functions by exploiting the specific binding between antibody-antigens[29]. An antibody (also immunoglobulin of Ig) is a glycoprotein that is secreted by plasma cells (specialized B lymphocytes)[30]. Antibodies are made of four polypeptides (2 heavy and 2 light chains) held together by disulfide and covalent bonds[30]. Different classes of Ig can have up to five structural molecules that can be combined to form one antibody. In mammals the classes are IgG, IgM, IgA, IgD and IgE, with further subdivision in the IgG and IgA group in some mammals; in birds the classes are IgY, IgM and IgA[30]. Because of the complex nature of antigens, antibody responses come in two main forms, monoclonal or polyclonal[30]. A polyclonal response is created by numerous lymphocytes recognizing different epitopes of an antigen and then proliferating and differentiating into plasma cells that will generate the antibody[30]. A monoclonal response is generated by a single B lymphocyte clone[30]. A monoclonal antibody is more specific, it may result in a higher level of false negatives, while a polyclonal antibody is more likely to recognize an epitope with less discernment for a specific antigen leading to more false positive results[31]. Using the indirect method, a primary antibody that is specific to an antigen (portion of a protein, ion channel etc.) is used as a probe to mark the target. Then an immunofluorescent secondary antibody that is sensitive to the species

and class of the primary antibody is used to visualize the antigen-antibody-antibody reaction under an immunofluorescent microscope[30,31].

In this study, the mice were trans-cardially perfused with 1x PBS followed by fixation of the tissues using 10% formalin. Tissues were cryoprotected in 30% sucrose and later embedded in gelatin for sectioning. The embedded brains were cut into 40µm sagittal sections and were stored in PBS with 1% sodium azide at 4 degrees, to be used for IHC analysis. IHC analysis used a permeabilization buffer of 0.3% Triton X-100 (a detergent) to break the cell wall and a blocking buffer of 15% normal goat serum NGS to prevent non-specific antibody binding. Primary antibodies used for tissue staining can be found in **TABLE 1.** Secondary staining was completed using polyclonal fluorophore-conjugated antibodies: goat anti-rabbit IgG Invitrogen 555 (thermos Fischer scientific) cy3, goat anti-mouse IgG Invitrogen 555 (thermos Fischer scientific) cy3, goat anti-chicken IgY Invitrogen 555 (thermos Fischer scientific) (1:750) cy3, goat anti-rabbit IgG Invitrogen 647 (thermos Fischer scientific) , goat anti-mouse IgG Invitrogen 647 (thermos Fischer scientific) (1:400), goat anti-chicken IgY Invitrogen 647 (thermos Fischer scientific). Nuclei were counterstained with 4', 6-Diamidino-2-phenylindole (DAPI, Molecular probes 1:1000) for 10 minutes after secondary antibody incubation. Tissues were then mounted on glass slides and dried overnight. The were cover slipped with Fluoromount G mounting medium (Thermo Fisher Scientific) for imaging.

Quantification and Microscopy

After staining the tissues collected, images of the cerebellum were captured using an Olympus BX61 confocal microscope (Olympus America Inc., Center Valley, PA). All images were taken within lobe IV/V, VI or VII The Calbindin and COXIV stain was taken at 60x magnification to obtain accurate mitochondrial puncta counts. The syntaphilin and neurofilament medium chain (NFM) images were taken at 10x in lobe IV/V and at 40x magnification. Unfortunately, due to poor tissue perfusion and cryoprotection, the puncta counts were inaccurate. The NeuN and GFAP stain was imaged at 10x magnification in lobe IV/V while the MBP and PV images were taken at 10x in lobe IV/V and 40x. Z-stack projections were obtained using Slidebook6 software. All images were post processed for equal exposure in slidebook. The images were then taken to ImageJ (NIH, Bethesda, MD for cell counts and analyses of the cerebellar cortex. For MBP density analysis, images were taken in lobe IV/V of the mouse cerebellum and regions of interest (ROI) were traced around the Purkinje cell layer on both sides of the lobe. The demyelination in the white matter was assessed by quantifying anti-MBP immunofluorescence intensity percent area around the ROIs. Puncta analysis of COXIV and Syntaphilin images was completed in accordance with lab protocol adapted from Horum et al., 2014. The ROIs were hand drawn around Purkinje neuron cell bodies to the best of the researchers ability. The image background was subtracted at a rolling ball radius of 50 pixels and the sliding paraboloid option was also selected. The CLAHE> EXP method was used to better isolate the puncta. From there the images were adjusted in brightness and contrast to improve puncta visibility and the threshold was

adjusted for analysis. These values were kept consistent within each animal line and stain.

Statistical analysis methods

Data analysis was conducted in Prism® (GraphPad, La Jolla) program for Windows. To assess a proper sample size to detect an effect of a given size with a given degree of confidence[27], a power analysis was completed prior to experimentation. The power is defined as the probability of being able to detect a specified effect, with a higher power being desired[27]. The power analysis determined that N=5 mice/group was sufficient for statistical power. Mitochondria puncta counts within the Purkinje cells were measured with Syntaphilin and COX4 stains. There were 3-5 mice per treatment group, and two sections per mouse/per treatment group were taken of the cerebellum for IHC. A one-way ANOVA was used to determine the association between treatment group and MBP percent area within each mouse line. The puncta count for syntaphilin and COXIV were analyzed using a Kruskal-Wallis test in conjunction with Dunns multiple comparisons test. Analysis was stratified by wild type and PCP2Cre + ERβ CKO samples. Differences were considered significant at the *$p<0.05$, **$p<0.01$, ***$p<0.001$, and ****$p<0.0001$ level. To compare the treatment groups of the WT to the PCP2Cre + ERβ CKO, a two-way ANOVA would need to be completed of the mean puncta counts and the MBP percent area. The two-way ANOVA allows for the analysis of the main effect of each independent variable (Transgenic mouse vs WT and Treatment group) to be considered in terms of the dependent variable (puncta count or percent area). Dunnett's

multiple comparisons test should be completed to determine differences within a specific treatment group.

Chapter 3: Results

EAE mice showed minimal change in MBP percent area.

Sagittal brain slices from day 40 EAE groups (normal, EAE+Vehicle, EAE+O-methyl) were subjected to IHC to assess white matter myelination in the cerebellum. Images were taken in cerebellar sections (lobe IV/V) that were stained with anti-MBP to determine the percent area. Using a 1-way ANOVA test white matter (WM) and granule cell layer (GCL) **FIG 1a.** were analyzed. Within the wild-type (WT) group, there were no significant differences between the three treatment groups **FIG 2**. However, for the PCP2Cre x Erβ CKO group, a statistically significant difference was found ($p= 0.0021$). Multiple comparisons using Tukey's post hoc tests showed a statistically significant difference between the normal and vehicle groups (mean difference = 7.65, 95% CI:3.309 ($p= 0.0016$)) and marginal significance between the EAE + vehicle and EAE+ O-methyl groups **Fig 2**.

Syntaphilin and COXIV puncta count.

Additional analysis to assess changes in mitochondria were completed via IHC. Cerebellar sections were stained with anti-Syntaphilin and anti-COXIV, to show approximate puncta counts of anchored and free-floating mitochondria. This helps us determine where the energetic needs of the cell reside. Syntaphilin and COXIV counts

were taken in the cell body of Purkinje neurons, **FIG 1b** and analyzed using a Kruskal-Wallis test. Within the WT group, a significant difference in median puncta count ($p=0.0007$) was found between the normal, EAE+Vehicle and EAE+ O-methyl groups. Multiple comparisons using Dunn's test reported a significant increase between the normal and O-methyl groups (adjusted $p = 0.0007$) and the EAE+vehicle and EAE+O-methyl group (0.0156) **Fig 3c.** No other significant associations were observed. The PCP2Cre+ ERβ CKO group was also tested using a Kruskal-Wallis test which showed significant differences within the groups ($p < 0.0001$). Dunn's Multiple comparisons test showed significant differences between the normal and vehicle group (adjusted $p = 0.0005$) **Fig 3c.** and significant differences between the EAE+vehicle and EAE+O-methyl groups (adj. $p = 0.0002$) **Fig 3c.**

COXIV mitochondrial puncta counts were also analyzed with a Kruskal-Walls test due to the nonparametric distribution of values. The analysis was stratified by WT and PCP2Cre + ERβ CKO samples. The Kruskal-Wallis test for the WT samples showed a statistically significant difference in mean rank between the three treatment groups. Dunn's multiple comparisons showed that puncta count for the EAE+ Vehicle group was significantly lower than that of the EAE+O-methyl group (adj. $p = 0.0278$) **Fig 4**. Within the PCP2Cre+ ERβ CKO samples, Kruskal- Wallis testing showed significant differences between the three treatment groups ($p = 0.0018$). Multiple comparisons showed significant differences between the normal and EAE+ vehicle groups (adj. $p = 0.0039$) and between the EAE+ vehicle and EAE+O-methyl group (adj. $p = 0.0071$) **Fig 4.**

Comparative analysis

To assess the effects of the PCP2Cre+ ERβ CKO in remyelination and PC health post ERβ ligand treatment, t-tests were completed to compare the EAE+O-Methyl treatment groups to each other. An unpaired t-test with Welch's corrections was used to determine if there was a significant difference between the EAE+O-Methyl WT and PCP2Cre+ ERβ CKO group. This analysis showed a significant difference ($p = 0.0458$) between the two groups, with the PCP2Cre + ERβ CKO group showing a significant decrease in MBP immunofluorescence intensity than the wild type of group ($p = 0.0145$)**.** The syntaphilin counts were analyzed using a Mann-Whitney t-test but showed no significant findings between the two groups.

Chapter 4: Discussion

The goal of this study was to examine if the ERβ ligand O-methyl acts directly or indirectly on the estrogen receptor. To do this, 23 mice (11 Wild Type, 12 PCP 2Cre+ ERβ CKO) were assigned to receive no treatment (Normal), EAE+Vehicle, or EAE with IndCl-O-methyl treatment. Tissues taken from these mice were imaged with slidebook6 and analyzed with ImageJ and Prism to process and quantify the immunofluorescence intensity of MBP (percent area) and mitochondrial puncta counts. Tissue samples without sufficient contrast in imaging were excluded from the final analysis. Regions of interest were identified via staining protocol and normal anatomical feature adjustment. Purkinje cell health was defined by mitochondrial puncta counts of syntaphilin and COXIV seen via IHC staining and overall cerebellar health was defined by the immunofluorescent intensity of the MBP (percent area).

The results of this study showed that MBP percent area in white matter and granule cell layer of the wild type mice was not significantly different between the three groups. This differs from the previous studies done by Atkinson et al. 2023 (paper under preparation) due to several reasons, most of all due to the poor tissue quality. In this experiment, the perfusion and subsequent cryoprotection was inadequate. In addition, brain slicing was not done well. This led to holes throughout the tissue, that made the analysis difficult to complete as accurately as possible. For this reason, the results gained from this study cannot be trusted. The experiment in its entirety will need to be repeated. Further study will need to be conducted to create accurate measurements of the MBP percent area

within the different treatment groups. The PCP2cre+ ERβ CKO data did show a significant difference within the three treatment groups, but upon further examination using multiple comparison tests it was discovered that the differences were only significant between the normal and EAE+O-methyl groups, with minimal significance between the EAE+Vehicle and EAE+ O-methyl groups (adj. p = 0.0693). Previous work from our lab and others have shown this demyelination in MOG EAE treated mice[8]. To compare the WT and PCP2Cre+ ERβ CKO EAE+O-methyl groups average MBP percent area, a Welch's t-test was completed. It showed a statistically significant difference between the two with the PCP2Cre + ERβ CKO samples showing lower MBP density. Under normal circumstances this could indicate that the remyelination activity of the ERβ ligand does require direct interaction between the receptor and the ligand, but due to the inconclusive nature of the intra-group data, this comparison would need to be repeated for further verification. A major limitation of this study was the small sample size. This resulted in high variance and affected the relative normality of the sample groups. This made it difficult to draw definitive conclusions about the myelin levels of the different treatment groups.

Syntaphilin functions as a mitochondrial anchor, while it is generally found in the axons of neurons, it does appear in other portions of the neuronal cell such as the synaptic space and cell body[18]. Postmortem studies of human MS patients showed higher expression of syntaphilin in demyelinated axons which is indicative of some form of protective mechanism that the cell takes when faced with demyelination[18]. In this study, we analyzed the cell bodies of the Purkinje neurons. While the role of syntaphilin is different

in the axon's vs the cell bodies, gathering puncta from the cell bodies does give an idea of how much energy is needed in other areas of the cell. Because the data was not normally distributed, a Kruskal-Wallis nonparametric data test was done. The WT data showed significant differences between the normal and EAE+ O-methyl groups, as well as the EAE+ Vehicle and EAE+O-methyl groups. Unfortunately, these results are inconclusive because there was no statistically significant differentiation between the normal and vehicle groups that had been seen in prior laboratory research Atkinson et. al, 2023 (paper under preparation). This data could indicate that mitochondria are moving to areas of greater energetic need, but without the validation of the change in disease state it is difficult to create conclusive evidence of this. The PCP2Cre+ ERβ CKO syntaphilin puncta however did show a significant difference between the Normal and EAE+ Vehicle groups, as well as between the EAE+ Vehicle and EAE+O-methyl group. This indicates that after EAE induction, the demyelination that is generated pulls mitochondria from the cell body. Further testing would need to be completed to verify where the mitochondria are going as well as their overall energetic levels. To see how the mitochondrial function is affected by the absence or presence of the beta estrogen receptor when treated with an ERβ ligand, a Mann-Whitney t-test was completed. This test did not show any significant differences between the two groups. This data will need to be re-configured due to the poor integrity of the wild type of tissue.

Another way that the mitochondria puncta were analyzed was with IHC of cytochrome C Oxidase (COX) subunit 4 (COXIV) puncta counts in Purkinje cell bodies. COXIV is the fourth protein complex of the electron transport chain and is a common biomarker for

mitochondria and its activity. The WT data of this study only showed significant differences in the EAE+ vehicle groups versus the EAE+ O-methyl group. Without the validation of change within the disease state, this finding is inconclusive. On the other hand, the PCP2cre+ ERβ CKO data showed a significant difference between the normal and vehicle as well as the EAE+ vehicle and EAE+ O-methyl groups. This data tells us that during EAE, the median number of mitochondrial increases, and the addition of the ERβ ligand aids in bringing these levels down to around normal. This increase in mitochondria seen could be due to several factors including fission of free-floating mitochondria to increase the overall energetics of a cell. To test the mitochondrial quantities with and without the estrogen receptor on the Purkinje cells a comparative one tailed Mann-Whiteny t-test was completed. This data did show significant differences between the WT and PCP2Cre+ ERβ CKO groups, with the WT having a higher median. Because of the poor tissue integrity, these studies will need to be repeated to draw any useful conclusions about the state of the mitochondria with and without the estrogen receptor.

Conclusion

In summary, this study has attempted to analyze changes in Purkinje cell and cerebellar health during EAE and with treatment of an ERβ ligand. While the data from this study did not show conclusive results, the work done here provides groundwork for further study by looking at myelination and mitochondria as a way of assessing PC status with and without the beta estrogen receptor. These experiments are currently being repeated

by the Tiwari-Woodruff lab, but due to time constraints I will not be able to redo these experiments. Further studies plan to redo these tests, and to do seahorse analysis to better understand the energetics of the mitochondria in these cells, as well as to do digital spatial profiling (DSP) to understand the proteomic and RNA sequences seen in lesioned areas.

Table 1: List of antibodies used.

ANTIBODY NAME	SOURCE	Vendor	LOT	CATALOG	Isotype
MBP	Chicken	EMD Millipore	3284364	AB9348	IgY
PV	Rb-poly	Sigma	000019368	HPA048536	IgG
Calbindin	MS-Mono	SIGMA	0000118423	C9848-2ML	IgG
COX IV	Rb-Poly	NOVUS	D-3	NB110-39115	IgG
Syntaphilin	Rb-poly	Invitrogen	VB2939345	PA5-20528	IgG
NFM	MS-Mono	EMD Millipore	MAB1621	3762523	IgG1
NeuN	Rb-poly	EMD Millipore	ABN78	3832723	unavailable
GFAP	Chicken	EMD Millipore	3877381	AB5541	unavailable

List of Figures

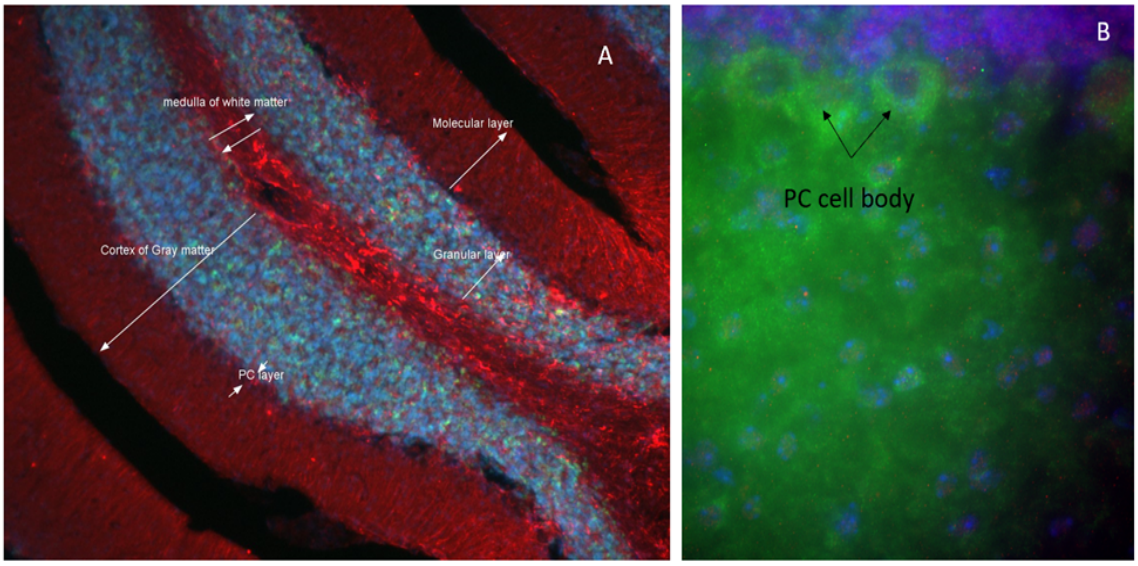

Figure 1: EAE mice showed minimal changes in optical MBP density (A) shows the different layers within the cerebellar lobes, stained with NeuN (green) GFAP (red) and Dapi (blue) at 10x magnification (B) Purkinje cell bodies stained with calbindin (green) and COXIV (red) taken at 60x magnification

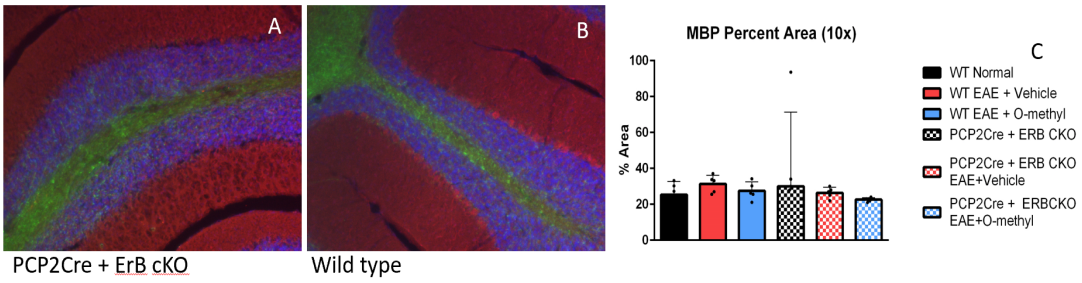

Figure 2: EAE mice showed minimal change in optical MBP density. (A) and (B) 10x representative images of normal mouse cerebellum taken at lobe IV/V stained with MBP (green), PV (red) and DAPI (blue). (C) MBP immunofluorescence intensity (percent area) analysis showed inconclusive results. The percent area change within the WT groups did not show any significance, and the error within the PCP2Cre + ErB cKO group was negligible due to the high variability within the normal groups

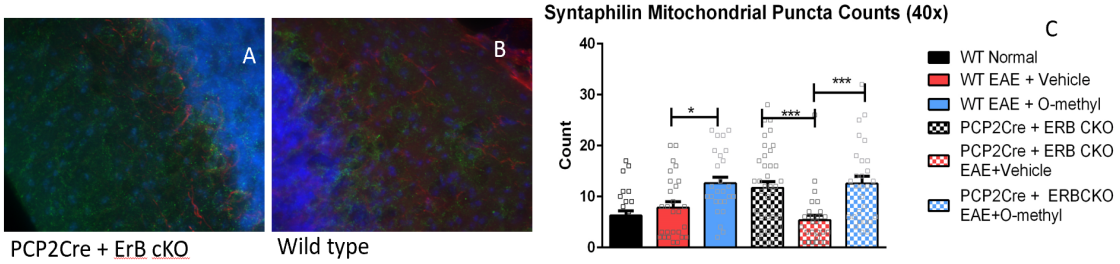

Figure 3: Syntaphilin puncta counts (A) a representative 40x image of the molecular, Purkinje and granule cell layers of the cerebellum at lobe IV/V stained with syntaphilin (green) NFM (red) and DAPI (blue) for the PCP2cre + Erb cKO mouse tissue (B) a 40x image in the same plane as A, of the wild type tissue. (C) a graphical representation of the puncta counts within each treatment group. Data are represented as mean ± SEM. * $p < .05$, *** $p < .001$

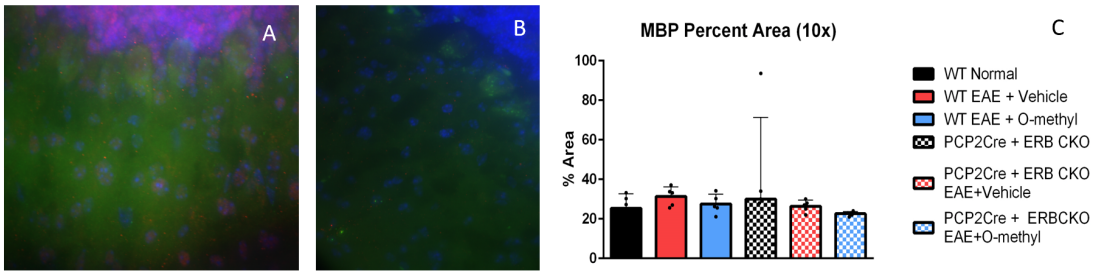

Figure 4: COXIV puncta counts (A) and (B): 60x representative images of Purkinje cell bodies in both the pcp2cre and wildtype (respectively) tissues stained with calbindin (green) COXIV (red) and DAPI (blue) **(C)** CoxIV puncta counts revealed no significant changes in the mitochondria of the cell bodies of Purkinje neurons but the PCP2Cre+ ErB cKO tissue had significant increase between the normal and vehicle treatment (adj. $p = 0.0039$) as well as a significant decrease between the EAE+ vehicle and the EAE+ O-methyl treated groups (adj. $p = 0.0071$). Data are represented as mean ± SEM. ** $p < .005$,

References

1. Maglione, A., Rolla, S., De Mercanti, S. F., Cutrupi, S. & Clerico, M. The adaptive immune system in multiple sclerosis: An estrogen-mediated point of view. *Cells* vol. 8 Preprint at https://doi.org/10.3390/cells8101280 (2019).
2. Walton, C. *et al.* Rising prevalence of multiple sclerosis worldwide: Insights from the Atlas of MS, third edition. *Multiple Sclerosis Journal* **26**, 1816–1821 (2020).
3. Hunter, S. F. Overview, and diagnosis of multiple sclerosis. *Am J Manag Care* **22**, s141-50 (2016).
4. Jimsheleishvili, S. & Dididze, M. *Neuroanatomy, Cerebellum*. (2023).
5. *Neuroscience*. (Sinauer Associates, 2001).
6. D'Angelo, E. & Casali, S. Seeking a unified framework for cerebellar function and dysfunction: from circuit operations to cognition. *Front Neural Circuits* **6**, (2013).
7. Palesi, F. *et al.* Contralateral cortico-ponto-cerebellar pathways reconstruction in humans in vivo: implications for reciprocal cerebro-cerebellar structural connectivity in motor and non-motor areas. *Sci Rep* **7**, 12841 (2017).
8. Atkinson, K. C., Osunde, M. & Tiwari-Woodruff, S. K. The complexities of investigating mitochondria dynamics in multiple sclerosis and mouse models of MS. *Frontiers in Neuroscience* vol. 17 Preprint at https://doi.org/10.3389/fnins.2023.1144896 (2023).
9. Wilkins, A. Cerebellar Dysfunction in Multiple Sclerosis. *Front Neurol* **8**, (2017).
10. Hafiz, S. & De Jesus, O. *Ataxia*. (2023).
11. Mattson, M. P., Gleichmann, M. & Cheng, A. Mitochondria in Neuroplasticity and Neurological Disorders. *Neuron* **60**, 748–766 (2008).
12. Yin, M. & O'Neill, L. A. J. The role of the electron transport chain in immunity. *The FASEB Journal* **35**, (2021).
13. Blagov, A. V., Sukhorukov, V. N., Orekhov, A. N., Sazonova, M. A. & Melnichenko, A. A. Significance of Mitochondrial Dysfunction in the Progression of Multiple Sclerosis. *Int J Mol Sci* **23**, 12725 (2022).
14. Mahad, D., Ziabreva, I., Lassmann, H. & Turnbull, D. Mitochondrial defects in acute multiple sclerosis lesions. *Brain* **131**, 1722–1735 (2008).
15. Wu, Y., Chen, M. & Jiang, J. Mitochondrial dysfunction in neurodegenerative diseases and drug targets via apoptotic signaling. *Mitochondrion* **49**, 35–45 (2019).
16. Kausar, S., Wang, F. & Cui, H. The Role of Mitochondria in Reactive Oxygen Species Generation and Its Implications for Neurodegenerative Diseases. *Cells* **7**, 274 (2018).

17. Trushina, E. & McMurray, C. T. Oxidative stress, and mitochondrial dysfunction in neurodegenerative diseases. *Neuroscience* **145**, 1233–1248 (2007).

18. Ohno, N. *et al.* Mitochondrial immobilization mediated by syntaphilin facilitates survival of demyelinated axons. *Proceedings of the National Academy of Sciences* **111**, 9953–9958 (2014).

19. Kipp, M., Nyamoya, S., Hochstrasser, T. & Amor, S. Multiple sclerosis animal models: a clinical and histopathological perspective. *Brain Pathology* vol. 27 123–137 Preprint at https://doi.org/10.1111/bpa.12454 (2017).

20. Praet, J., Guglielmetti, C., Berneman, Z., Van der Linden, A. & Ponsaerts, P. Cellular and molecular neuropathology of the cuprizone mouse model: Clinical relevance for multiple sclerosis. *Neurosci Biobehav Rev* **47**, 485–505 (2014).

21. Hasselmann, J. P. C., Karim, H., Khalaj, A. J., Ghosh, S. & Tiwari-Woodruff, S. K. Consistent induction of chronic experimental autoimmune encephalomyelitis in C57BL/6 mice for the longitudinal study of pathology and repair. *J Neurosci Methods* **284**, 71–84 (2017).

22. Karim, H. *et al.* Analogues of ERβ ligand chloroindazole exert immunomodulatory and remyelinating effects in a mouse model of multiple sclerosis. *Sci Rep* **9**, 503 (2019).

23. Confavreux, C., Hutchinson, M., Hours, M. M., Cortinovis-Tourniaire, P. & Moreau, T. Rate of Pregnancy-Related Relapse in Multiple Sclerosis. *New England Journal of Medicine* **339**, 285–291 (1998).

24. Kim, S., Liva, S. M., Dalal, M. A., Verity, M. A. & Voskuhl, R. R. Estriol ameliorates autoimmune demyelinating disease: Implications for multiple sclerosis. *Neurology* **52**, 1230–1230 (1999).

25. MacKenzie-Graham, A. *et al.* Purkinje cell loss in experimental autoimmune encephalomyelitis. *Neuroimage* **48**, 637–651 (2009).

26. Mangiardi, M. *et al.* An Animal Model of Cortical and Callosal Pathology in Multiple Sclerosis. *Brain Pathology* **21**, 263–278 (2011).

27. Hasselmann, J. P. C., Karim, H., Khalaj, A. J., Ghosh, S. & Tiwari-Woodruff, S. K. Consistent induction of chronic experimental autoimmune encephalomyelitis in C57BL/6 mice for the longitudinal study of pathology and repair. *J Neurosci Methods* **284**, 71–84 (2017).

28. Karim, H. *et al.* Analogues of ERβ ligand chloroindazole exert immunomodulatory and remyelinating effects in a mouse model of multiple sclerosis. *Sci Rep* **9**, (2019).

29. Magaki, S., Hojat, S. A., Wei, B., So, A. & Yong, W. H. An Introduction to the Performance of Immunohistochemistry. in 289–298 (2019). doi:10.1007/978-1-4939-8935-5_25.

30. Lipman, N. S., Jackson, L. R., Trudel, L. J. & Weis-Garcia, F. Monoclonal Versus Polyclonal Antibodies: Distinguishing Characteristics, Applications, and Information Resources. *ILAR J* **46**, 258–268 (2005).

31. Guerin, C. J. Using Antibodies in Microscopy: A Guide to Immunohistochemistry. Part 2: IHC Staining Protocols. *Micros Today* **31**, 34–39 (2023).